Journal of Alloys and Compounds 504 (2010) 60–64

Contents lists available at ScienceDirect

Journal of Alloys and Compounds

journal homepage: www.elsevier.com/locate/jallcom

Dependency of microhardness on solidification processing parameters and microstructure characteristics in the directionally solidified Ti–46Al–0.5W–0.5Si alloy

Jianglei Fan*, Xinzhong Li, Yanqing Su, Jingjie Guo, Hengzhi Fu

School of Material Science and Engineering, Harbin Institute of Technology, Harbin, Heilongjiang 150001, PR China

ARTICLE INFO

Article history:
Received 6 March 2010
Received in revised form 14 May 2010
Accepted 21 May 2010
Available online 1 June 2010

Keywords:
Titanium aluminide
Directional solidification
Microhardness
Intermetallics

ABSTRACT

TiAl-based alloy (Ti–46Al–0.5W–0.5Si at.%) was directionally solidified at a constant temperature gradient (G = 20 K/mm) in a wide range of growth rates (2–100 μm/s) by using a Bridgman type directional solidification furnace. The dendritic spacing (λ), lamellar spacing (λ_L) and microhardness (H_V) were measured. The value of H_V increases with the increasing growth rate (V) and decreases with the increasing dendritic spacing and interlamellar spacing. The dependence of H_V on V, λ and λ_L was determined by linear regression analysis. The relationships between the V and H_V, and λ and H_V, and λ_L and H_V were given as $H_V = 794.7V^{0.15}$, $H_V = 398.1\lambda^{-0.31}$ and $H_V = 491.5 + 53.4\lambda_L^{-0.5}$, respectively. The fitted exponent values obtained in this work were compared with the previous similar experimental results.

1. Introduction

Intermetallic γ-TiAl based alloys are considered to be attractive candidate materials for high temperature structural applications in aerospace and automotive industries due to their low density, good oxidation resistance and high temperature strength [1–4]. Of the numerous microstructures that can be formed in TiAl-based alloys, the fully lamellar microstructures consisting of TiAl (γ phase) and Ti_3Al (α_2 phase) have displayed a good combination of room temperature toughness and elevated temperature strength [5]. However, initial application of TiAl alloys was limited by major obstacles such as the low room-temperature ductility, the difficulty in processing then to fabricate a component and poor oxidation resistance above 800 °C [1–4]. Efforts have been focused on refining the grain size by controlling of microstructures and improve the mechanical properties by alloying additions of B, Si, W, Cr, V, Mn and Mo. Small additions of B and W have been shown to refine the lamellar structure in TiAl alloys [6].

During the last two decades, intensive works have been carried out in the field of directional solidification using a seeding technique, in order to achieve a columnar grain material with the lamellar orientation aligned parallel to the growth direction and thus a good combination of strength, ductility and fracture toughness [7–9].

Presently, most efforts are concentrated on TiAl-based alloys with various alloying additions [7,10–16]. Alloying elements, such as W, Ta, Nb or Si, are usually added to improve high temperature resistance and lamellar structure stability. Thus, several alloy compositions have been developed to meet specific property requirements, e.g. Ti–48Al–2Nb–2Cr (at.%) [13] alloy for maximum room temperature ductility and Ti–47Al–2W–0.5Si (at.%) alloy for maximum creep resistance [14,16,17]. Tungsten is known to act most effectively as solid solution strengthener and stabilizer of β phase [11]. Small addition of silicon improves high-temperature oxidation resistance; especially the fine coherent Ti_5Si_3 particles formed through eutectoid reaction along lamellar interfaces enhance creep resistance [7,11,14,17,18]. Coarse Ti_5Si_3 particles maybe precipitate directly from liquid that reduces the tensile properties greatly [19]. The present work deals with directional solidification experiments performed on a quaternary Ti–46Al–0.5W–0.5Si (at.%) alloy. This composition slightly deviates from the well-known Ti–46Al–2W–0.5Si (at.%) alloy developed for investment cast turbine blades by reduction of content of W.

Lapin et al. [11,20] has reported that there is a linear relationship between yield stress and microhardness, which allows mechanical properties of directionally solidified TiAl ingots to be predicted from the values of Vickers microhardness. Similar linear dependence of the yield stress on the hardness was observed in wrought Ti–45.3Al–2.1Cr–2.0Nb (at.%) alloy with fully lamellar structure [21]. It appears that the microhardness analysis presented offers a relatively simple way to accomplish the complex task of predicting mechanical properties of materials [22]. The values of Vickers

* Corresponding author. Tel.: +86 0451 86418815; fax: +86 0451 86415776.
E-mail address: JLFan2011@163.com (J. Fan).

0925-8388/$ – see front matter © 2010 Elsevier B.V. All rights reserved.
doi:10.1016/j.jallcom.2010.05.095

Table 1
Chemical composition of Ti–46Al–0.5W–0.5Si (at.%) alloy O.

Element	Ti	Al	W	Si	O	Other
at.%	Balance	45.27	0.62	0.52	0.05	<0.1

microhardness are useful for quality control in the production of TiAl alloys.

The microhardness is sensitive to chemical composition, solidification processing parameters (such as temperature gradient (G) and growth rate (V)) and microstructure parameters (such as dendritic spacing (λ), interlamellar spacing (λ_L) and the spatial and size distributions of the phases) [22,23]. The Hall–Petch type relationships between the microhardness (H_V), V, λ and λ_L were observed on the logarithmic scales. The Hall–Petch type relationships can be expressed as follows [23],

$$H_V = H_0 + k_1 V^b \quad (1)$$

$$H_V = H_0 + k_2 \lambda^{-d} \quad (2)$$

where b and d are exponent values for the growth rate and the dendritic spacing, respectively, and H_0, k_1 and k_2 are constants. The Hall–Petch type relationship can be rewritten as follows [23]:

$$H_V \approx k_1 V^b \quad (3)$$

$$H_V \approx k_2 \lambda^{-d} \quad (4)$$

In this paper, Ti–46Al–0.5W–0.5Si (at.%) has been carried out to experimentally investigate the dependence of the microhardness (H_V) on the growth rate (V), dendritic spacing (λ) and interlamellar spacing (λ_L) during the directional solidification.

2. Experiments

Master ingot with nominal composition of Ti–46Al–0.5W–0.5Si (at.%) alloy was prepared by using Ti (99.96%), Al (99.99%), W (99.98%), and Si (99.96%) of commercial purity in a cold crucible induction furnace under argon atmosphere. Chemical composition of the alloy was analyzed by spectral analysis, as shown in Table 1. The samples were machined to rods with 3 mm diameter and 100 mm in length from the ingot by a spark machining. The directional solidification (DS) experiments were performed in a Bridgman-type system, consisting of an resistance furnace, a water cooled liquid metal bath filled with a liquid Ga–In–Sn alloy, and an adiabatic zone which is located between the heater and the cooler, as previously described in Ref. [24]. The temperature gradient was measured by W/Re thermocouples that were placed near the outside surface of the alumina tubes. One thermocouple was placed about 5 mm from the bottom of the sample where is near the solid–liquid interface. Other was placed approximately 15 mm from the bottom of the sample where is the liquid region. The temperature gradient close to the solid/liquid interface was measured to be approximately 20 K/mm. The samples are placed into 99.99 pct pure alumina crucibles of 4/5.5 mm diameter (insider/outside diameter) and length of 150 mm. After 4 h heating to 1773 K and 30 min temperature stabilization, the sample was pulled at a selected velocity from 2 to 100 μm/s.

The longitudinal and transverse section of the specimens were cut, polished and etched with a solution of 10 ml HF–10 ml HON_3–180 ml H_2O for further analysis. After metallographic process, the microstructures of the samples were revealed and photographed with optical microscope. Fig. 1 shows the typical images of optical microscope.

The dendritic spacings were measured from the photographs according to the method described in Refs. [23,25]. The interlamellar spacings were measured from the SEM back scattered electron (BSE) images according to the method described in Ref. [26]. The value of interlamellar spacing is the thickness of one α lamellae and γ lamellae nearby. Fig. 2 shows the typical BSE image of lamellar structures. The measured values of the dendritic spacings and interlamellar spacings are the average values and given in Table 2.

Microhardness measurements were made with a standardized Vickers measuring test device using 100 g load and a dwell time of 10 s on the transverse section. The Microhardness is average of at least 15 measurements. The values of H_V are also given in Table 2.

3. Results and discussion

Ti–46Al–0.5W–0.5Si (at.%) alloy were directionally solidified with a constant temperature gradient (G = 20 K/mm) at different growth rates (V = 2–100 μm/s) in order to see the dependence of H_V on the V, λ and λ_L. The microstructures of the directionally solidified specimen consisted of α_2/γ lamellar structures and Ti_5Si_3 phases, as shown in Fig. 2. The black phase is γ (TiAl) phase, the gray one is α_2 (Ti_3Al) phase and the white is Ti_5Si_3 phase. The lamellar structures formed by eutectoid reaction: $\alpha \rightarrow \alpha_2 + \gamma$. In addition, some Al_2O_3 particles that formed by the reaction between the crucible and the alloy were observed at the end part of the directionally solidified specimens, as shown in Fig. 2.

Table 2
The values of dendritic spacing, lamellar spacing and microhardness for directionally solidified Ti–46Al–0.5W–0.5Si (at.%) alloy at various growth rate with constant temperature gradient (G = 20 K/mm).

Solidification parameters		Dendritic spacing λ (μm)	Lamellar spacing λ_L (μm)	Microhardness H_V
G (K/mm)	V (μm/s)			
20	2	–	4.22	326.2
	3	–	4.18	330.6
	5	–	4.01	354.1
	8	–	3.8	400.1
	10	971.7	3.61	410.4
	15	860.3	3.49	419.6
	20	762.4	3.21	443.3
	25	631.7	3.32	440.2
	30	630.8	2.95	426.4
	40	663.4	2.9	478.9
	50	570.7	2.81	510.5
	60	467.5	2.80	496.2
	70	380.3	2.78	537.8
	80	360.0	2.70	566.9
	90	281.9	2.74	573.6
	100	314.2	2.54	614.6

The values of dendritic spacing at growth rates from 2 to 8 μm/s were not measured because that the solid–liquid interface are cellular interface for these growth rates.

3.1. Dependency of the microhardness on the growth rate

In Table 2, the largest H_V was obtained at the maximum growth rate (V = 100 μm/s) and the smallest H_V was obtained at the minimum growth rate (V = 2 μm/s). The variations in the microhardness (H_V) with the growth rate (V) at a constant temperature gradient (G = 20 K/mm) are shown in Table 2 and Fig. 3. The error bars indicate the errors in the H_V values, which are in the range of ±1%. The value of H_V increases with the increasing the values of V at constant G. The relationship between H_V and V was obtained by using linear regression analysis, the results were given as:

$$H_V = 794.7\, V^{0.15} \quad (5)$$

The regression coefficient of this fit is r^2 = 0.97.

The exponent value has been compared with the exponent values obtained in previous works [11] for the similar solidification conditions in different alloy systems. The exponent value of growth rate (V) is 0.15 that is in good agreement with 0.14 obtain by Lapin et al. [11] for Ti–46Al–2W–0.5Si (at.%) alloy. The values of H_V are lower than those measured by Lapin [20] corresponding to different growth rate for directionally solidified Ti–46Al–2W–0.5Si (at.%) alloy. Different exist in the values of H_V may due to the difference in solidification condition and the amount of Al_2O_3 particles which can improve mechanical properties [27].

3.2. Dependency of the microhardness on the dendritic spacing

The variations in the microhardness (H_V) with the dendritic spacing (λ) at a constant temperature gradient (G = 20 K/mm) are shown in Table 2 and Fig. 4. The error bars indicate the errors in the H_V values and λ values, which are in the range of ±1% and ±2%, respectively. The value of H_V decreases with the increasing

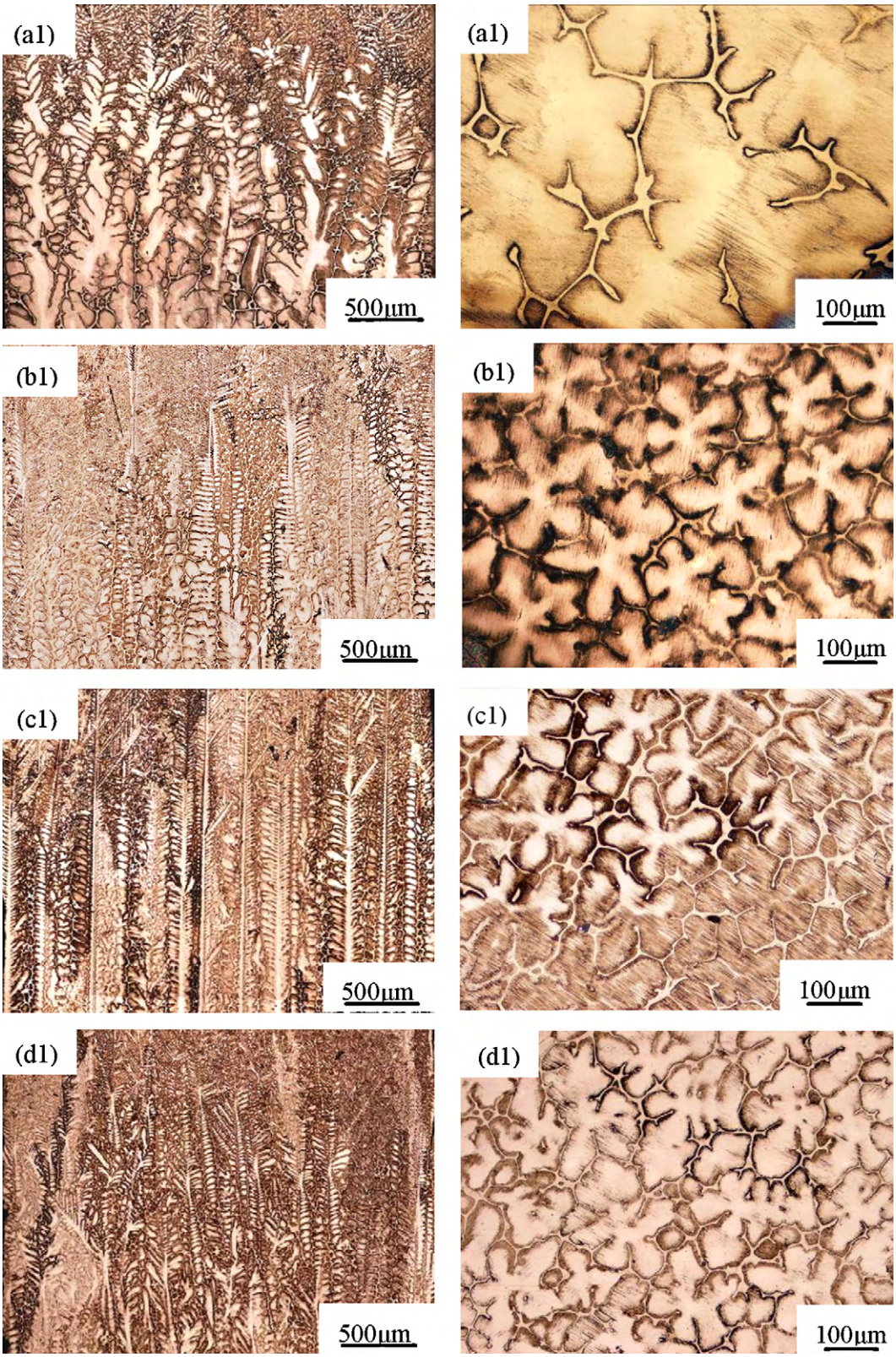

Fig. 1. Typical optical images of growth morphologies of directionally solidified Ti–46Al–0.5W–0.5Si (at.%) alloy with different growth rates at a constant gradient (20 K/mm): (a) $V = 10$ μm/s; (b) $V = 30$ μm/s; (c) $V = 70$ μm/s; (d) $V = 90$ μm/s; the left sides are corresponded to longitudinal section, right side corresponded to transverse microstructures, respectively.

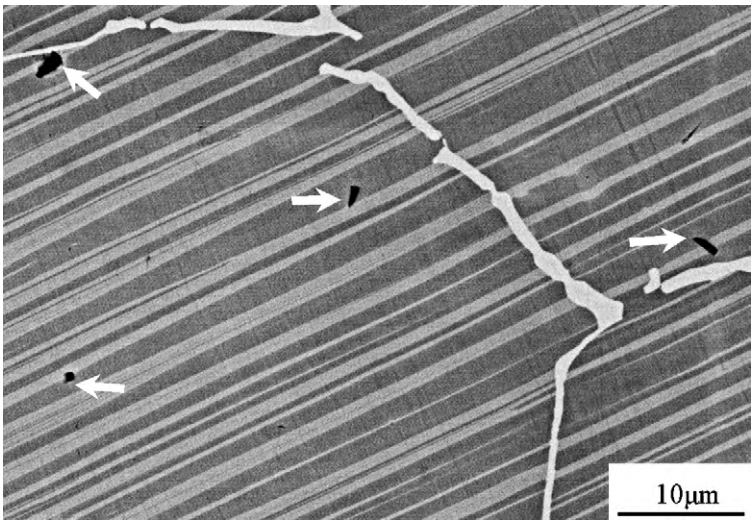

Fig. 2. BSE micrograph shows a typical microstructure of the directionally solidified Ti–46Al–0.5W–0.5Si (at.%) on the transverse section at growth rate of 30 μm/s. The black phase is γ phase, the grain phase is α_2 phase and the bright phase is Ti_5Si_3 phase. The arrows indicate the Al_2O_3 particles.

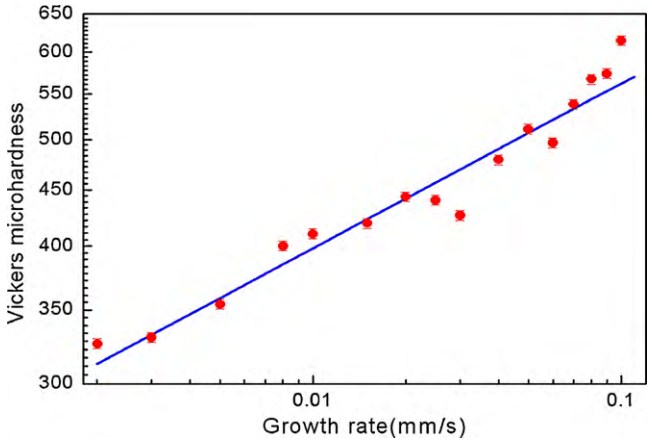

Fig. 3. Variation of microhardness as a function of growth rate for directionally solidified Ti–46Al–0.5W–0.5Si (at.%) alloy at a constant temperature gradient (G = 20 K/mm).

the value of λ at constant G. The relationship between H_V and λ was obtained by using linear regression analysis, the results were given as:

$$H_V = 398.1\,\lambda^{-0.31} \quad (6)$$

The regression coefficient of this fit is r^2 = 0.94.

3.3. Dependency of the microhardness on the interlamellar spacing

The variations of the microhardness (H_V) with the interlamellar spacing (λ_L) at a constant temperature gradient (G = 20 K/mm) are shown in Table 2 and Fig. 5. The error bars indicate the errors in the H_V values, which are in the range of ±1%. The value of H_V increases with the increasing the value of $\lambda_L^{-0.5}$ at constant G. The values of H_V were fitted to a Hall–Petch type relationship in the form of $H_V = H_{V0} + k\lambda_L^{-0.5}$ [11], where H_{V0} and k are materials constants. The relationship between H_V and $\lambda_L^{-0.5}$ was obtained by using linear regression analysis, the results were given as:

$$H_V = 491.5 + 53.4\,\lambda_L^{-0.5} \quad (7)$$

The regression coefficient of this fit is r^2 = 0.96.

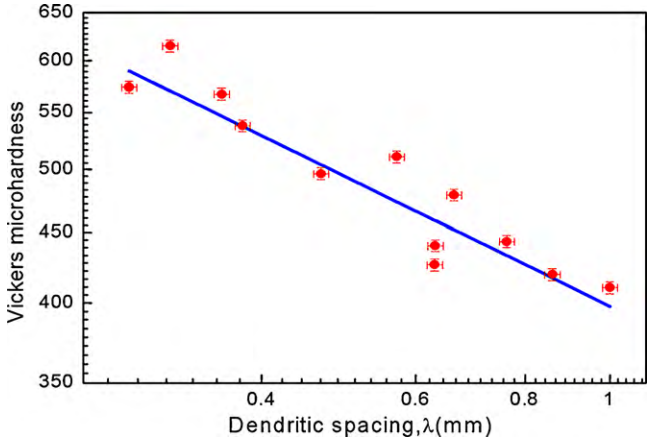

Fig. 4. Variation of microhardness as a function of dendritic spacing for directionally solidified Ti–46Al–0.5W–0.5Si (at.%) alloy at a constant temperature gradient (G = 20 K/mm).

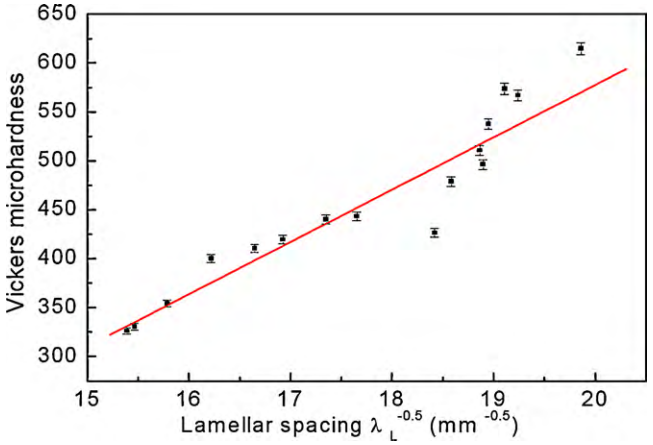

Fig. 5. Variation of microhardness as a function of the reciprocal square root of mean interlamellar spacing for directionally solidified Ti–46Al–0.5W–0.5Si (at.%) alloy at a constant temperature gradient (G = 20 K/mm).

4. Conclusions

In the present work, Ti–46Al–0.5W–0.5Si (at.%) alloy was directionally solidified with a constant temperature gradient ($G = 20$ K/mm) and growth rates ranging from 2 to 100 μm/s by using a Bridgman type directional solidification furnace. The value of microhardness (H_V) increases with increasing growth rate (V). The value of H_V increases with decreasing dendritic spacing (λ) and α–γ interlamellar spacing (λ_L) according to the Hall–Petch type relationships. The relationship between these parameters were given as, $H_V = 794.7V^{0.15}$, $H_V = 398.1\lambda^{-0.31}$, and $H_V = 491.5 + 53.4\lambda_L^{-0.5}$, respectively.

Acknowledgments

This project was supported by National Science Foundation of China (Nos. 50771041 and 50801019) and Post-doctor Foundation of China (No. 20080430909).

References

[1] X. Wu, Intermetallics 14 (2006) 1114–1122.
[2] H. Clemens, H. Kestler, Adv. Eng. Mater. 2 (2000) 551–570.
[3] D.M. Dimiduk, Mater. Sci. Eng. A263 (1999) 281–288.
[4] Y.W. Kim, JOM (1994) 30.
[5] D.R Johnson, H. Inui, M. Yamaguchi, Acta Mater. 44 (1996) 2523–2535.
[6] D.J. Larson, C.T. Liu, M.K. Miller, Intermetallics 5 (1997) 497–500.
[7] D.R. Johnson, H. Inui, S. Muto, Y. Omiya, T. Yamanaka, Acta Mater. 54 (2006) 1077–1085.
[8] D.R. Johnson, Y. Masuda, H. Inui, M. Yamaguchi, Acta Mater. 45 (1997) 2523–2533.
[9] D.R. Johnson, Y. Masuda, H. Inui, M. Yamaguchi, Mater. Sci. Eng. A239–240 (1997) 577–583.
[10] S.W. Kim, K.S. Kumar, M.H. Oh, D.M. Wee, Intermetallics 15 (2007) 976–984.
[11] J. Lapin, L. Ondrúš, M. Nazmy, Intermetallics 10 (2002) 1019–1031.
[12] T. Yamanaka, D.R. Johnson, H. Inui, M. Yamaguchi, Intermetallics 7 (1999) 779–784.
[13] G.E. Fuchs, Mater. Sci. Eng. A192–193 (1995) 707–715.
[14] W.M. Yin, V. Lupinc, L. Battezzati, Mater. Sci. Eng. A239–240 (1997) 713–721.
[15] B.G. Kim, G.M. Kim, C.J. Kim, Scr. Metall. Mater. 33 (1995) 1117–1125.
[16] W.M. Yin, V. Lupinc, Scr. Mater. 37 (1997) 211–217.
[17] R. Yu, L.L. He, Z.X. Jin, J.T. Guo, H.Q. Ye, V. Lupinc, Scr. Mater. 44 (2001) 911–916.
[18] R. Yu, L.L. He, J.T. Guo, H.Q. Ye, V. Lupinc, Acta Mater. 48 (2000) 3701–3710.
[19] M. Nazmy, M. Staubi, Scri. Metall. Mater. 31 (1994) 829–833.
[20] J. Lapin, J. Mater. Sci. Lett. 22 (2003) 747–749.
[21] D.M. Dimiduk, P.M. Hazzledine, T.A. Parthasarathy, S. Seshagiri, M.G. Mendiratta, Metall. Mater. Trans. A 29 (1998) 37–47.
[22] P. Christodoulou, M. Garbiak, B. Piekarski, Mater. Sci. Eng. A457 (2007) 360–367.
[23] H. Kaya, M. Gündüz, E. Çadırlı, N. Maraşlı, J. Alloys Compd. 478 (2009) 281–286.
[24] L.S. Luo, Y.Q. Su, J.J. Guo, X.Z. Li, S.M. Li, H. Zhong, L. Liu, H.Z. Fu, J. Alloys Compd. 461 (2008) 121–127.
[25] U. Böyük, N. Maraşlı, J Alloys Compd. 485 (2009) 264–269.
[26] E. Çadırlı, H. Kaya, M. Gündüz, Mater. Res. Bull. 38 (2003) 1457–1476.
[27] J. Lapin, L. Ondrúš, O. Bajana, Mater. Sci. Eng. A360 (2003) 85–95.